Photo-oxidation of ethylene over mesoporous TiO₂/SiO₂ catalysts

A. Licciulli [1](*), R. Nisi [1], S. Pal [1], A. M. Laera [1], P. Creti [2], A. Chiechi [3]

[1] *Dipartimento di Ingegneria dell'Innovazione, Università di Salento, Via Arnesano, 73100 Lecce, Italy.*
[2] *CNR Istituto Microelettronica e Microsistemi, Sezione di Lecce, 73100 Lecce, Italy.*
[3] *Salente SRL, Via Monteroni 147, 73100 Lecce, Italy.*

Abstract: Mesoporous TiO₂/SiO₂ catalysts were prepared in order to increase the post-harvest life of climacteric fruits and vegetables reducing ethylene concentration by photo-oxidation. TiO₂/SiO₂ powders were synthesized by sol-gel method using titanium isopropoxide Ti(O^iPr)₄ and tetraethoxysilane Si(OC₂H₅)₄ as source of metal oxides. Mesoporous SiO₂ framework was used as catalyst support of nanostructured TiO₂ to enhance the photocatalytic efficiency. Different TiO₂/SiO₂ molar ratios were prepared through sol-gel process. A liquid-crystal template route allowed to obtain the mesoporous silica structure, and contemporary TiO₂ insertion in the silica framework. The X-ray diffraction (XRD) analysis demonstrated that silica insertion in TiO₂ framework inhibits the anatase to rutile phase transformation at higher sintering temperature. The photocatalytic efficiency of the catalysts was measured by the photo-oxidation of ethylene gas under UV light irradiation. Complete photo-oxidation of ethylene was observed after 24 h of reaction time. Results show that the silica framework increases the surface area of the composites and make crystalline anatase phase more stable at higher temperature.

1. Introduction

Ethylene gas (C_2H_4) is the ripening hormone of several fruits and vegetables (Hussain *et al.*, 2011; Keller *et al.*, 2013). Ethylene is used to promote the uniform ripening of immature fruits such as bananas, but in most cases it doesn't work as beneficial element both in food and horticultural industries. Few ppm of ethylene in the storage atmosphere induce very fast ripening in postharvest which causes undesirable product losses (Keller *et al.*, 2013). Thus it is desired to remove or degrade ethylene from the storage environment in order to preserve the postharvest products and keep them fresh for a longer time period. The important role of ethylene as growth regulator of climacteric products was intensively investigated in the last 50 years and now the ripening process associated to high ethylene production is well known. Various methods to remove ethylene have been developed: ventilation, or controlled atmosphere, ethylene oxidation using potassium per-manganate. The photocatalytic ethylene oxidation thus represents an innovative way to extend postharvest life of the climacteric fruits and vegetables (Park *et al.*, 2009; Keller *et al.*, 2013; Ye *et al.*, 2013). Among the catalysts able to induce ethylene photo-oxidation, TiO_2 is promising and attractive due to low cost, non-toxicity and high efficiency. The photocatalytic properties of nanostructured TiO_2 have already been highlighted in several applications, such as photocatalytic degradation of both air and water organic pollutants, and self-cleaning surface protection (Pal *et al.*, 2014).

Anchoring TiO_2 nanocrystals on suitable mesoporous substrate brings relevant practical advantages. The immobilization on support materials slows or totally inhibits nanoparticles coarsening, preserving their higher surface area. Secondly, the substrate greatly improves handling, processing and recover of TiO_2 nanopowder. Mesoporous silica, as a catalyst support over nano-sized TiO_2, represent a good choice due to high specific surface area and improved thermal stability of the TiO_2 anatase crystalline phase. Some recent works also demonstrated higher photocatalytic activity of TiO_2/SiO_2 mixed oxide composites (Fu *et al.*, 1996; Zhan *et al.*, 2014).

The mesoporous SiO_2 is able to reduce the recombination of photogenerated electron-hole pair, while higher surface area increases the efficiency in the heterogeneous photocatalysis.

Over the past thirty years a successful synthetic strategy, named liquid-crystal template, leading to mesoporous materials has been developed allowing to finely tune the porosity (Corma *et al.*, 2006; Xiao *et al.*, 2008). This methodology involves supramolecular aggregates of ionic surfactants that act as templating agents, which are able to direct and control the crystallization of the inorganic nanoparticles (Beck *et al.*, 1992). After the surfactant removal by thermal annealing, mesoporous solids with high surface area can be obtained. The morphological and structural properties of the products can be finely tuned by varying process parameters such as pH, temperature, reagent concentrations, surfactants and silica sources.

In this work, TiO_2/SiO_2 binary composites obtained through a liquid-crystal template methodology have been tested as catalyst in UV light assisted ethylene oxidation at room temperature for the application in modified atmosphere packaging of climacteric fruits and vegetables. A titania precursor was added in the reaction medium containing the surfactant and the silica source allowing the one-pot formation of TiO_2 and SiO_2. Structure and morphology of the obtained TiO_2/SiO_2 binary composites with several weight ratios were investigated by using Brunauer-Emmett-Teller (BET) surface area, X-ray diffraction (XRD), Fourier transform infrared spectroscopy (FTIR) and Field emission scanning electron microscopy (FESEM) measurements.

2. Materials and Methods

Synthesis of TiO_2/SiO_2 binary oxides

All the reagents involved in the catalyst synthesis were purchased from Sigma Aldrich and were used without any further modification. The starting colloidal solution was obtained by dissolving 28 g of Pluronic F127 ($EO_{106} PO_{70} EO_{106}$) in 150 g of distilled water through vigorous stirring. The complete polymer dissolution was reached after addition of a solution of 2M HCl (600 g). Then the required amount of tetraethoxysilane [$Si(OC_2H_5)_4$, TEOS] was added drop wise and continued to stirring for an hour. At this stage, titanium tetraisopropoxide [$Ti(O^iPr)_4$, TTIP] was slowly added and stirred for overnight. The obtained reaction mixture was heated at 100°C for 24 h and after that, a xerogel was obtained by centrifuging. The xerogel was then dried and calcined at 550°C for 6 h with the heating and cooling rate of 1°C/min to remove the organic content. Following this procedure, binary oxide with the TiO_2/SiO_2 weight ratio of 9/1, 8/2, and 7/3 were prepared. For comparison, a sample of pure TiO_2 was also prepared with the same experimental condition. Throughout the text, these samples are represented as TSBA-10, TSBA-91, TSBA-82, and TSBA-73, respectively.

Characterization

Crystalline phases of the TiO_2/SiO_2 powder samples were characterized by X-ray diffraction (XRD) performed on a Rigaku Ultima X-ray diffratometer using Cu$K\alpha$ radiation ($\lambda=1.5406$ Å) operating at 40 kV/30 mA with the step size of 0.02°. FTIR spectra of the obtained composites were carried out with a JASCO FTIR-6300 over the range 4000-400 cm^{-1} with a resolution of 4 cm^{-1} and accumulating 256 scans for each measurement adopting KBr disc method. Specific surface area of the samples was measured by BET method using a Quantachrome NOVA 2200e surface analyzer. FESEM measurements were performed with a Zeiss scanning electron microscope.

Photocatalytic experimental set up

Photo-oxidation of ethylene gas under UV irradiation in the presence of TiO_2/SiO_2 composite powder samples was performed inside a photocatalytic reactor consisting of a quartz tube of 3L irradiated by 4 UV light sources (Osram Puritec HNS15WG13, 15W, emitting at 254 nm). The pictures of the catalytic reactor have been reported in figure 1. The experimental set up was equipped with flowmeters, vacuum pump, diaphragm pump for gas recirculation, and thermocouples for the temperature control inside the reactor. The TiO_2/SiO_2 powder samples (3 g) were placed in the quartz tube on a rectangular quartz vessel. Before filling the reactor with ethylene gas/air atmosphere, it was kept in vacuum to ensure the purity inside the chamber. Then a gas mixture of air and ethylene (1 equivalent %) was introduced in the reactor with a controlled flow system. All the experiments were performed at atmospheric pressure and the purged gas was continuously circulated in a closed circuit while maintaining room temperature inside the reactor. Ethylene photo-oxidation was monitored at regular intervals by using an Agilent Gas Chromatograph 7820 A equipped with a capillary column (HP-PLOT/Q).

Fig. 1 - Pictures of the experimental set-up reactor for evaluating photocatalysis efficiency.

Fig. 2 - Pore size distribution curve of (A) the mesoporous silica (SBA) and (B) TiO₂ (TSBA-10).

3. Results and Discussion

To investigate the effect of silica framework and mesoporosity in the catalyst nanostructure, BET specific surface area measurements were performed on the powder samples. BET measurements showed an increase in specific surface area with the increase in silica content. The sample SBA of pure silica represents pores with an average diameters of 3.4 nm and a specific surface area of ~553 m²/g, while the pure TiO₂ (TSBA-10) has pores with average diameter of 16.7 nm and a specific surface area of ~59 m²/g. A great ratio of surface/volume is a crucial parameter to optimize photocatalytic efficiency of nanostructered semiconductors. Intermediate values of specific surface area and average diameters between those recorded for pure silica and TiO₂, have been obtained on the binary TiO₂/SiO₂ oxides (Fig. 2).

The phase transformation of the TiO₂/SiO₂ catalysts was investigated by XRD and the spectra of each sample are presented in figure 3. The average crystalline size was estimated according to the Scherrer's equation, accounting the most intense diffraction peaks of the corresponding anatase and rutile phases.
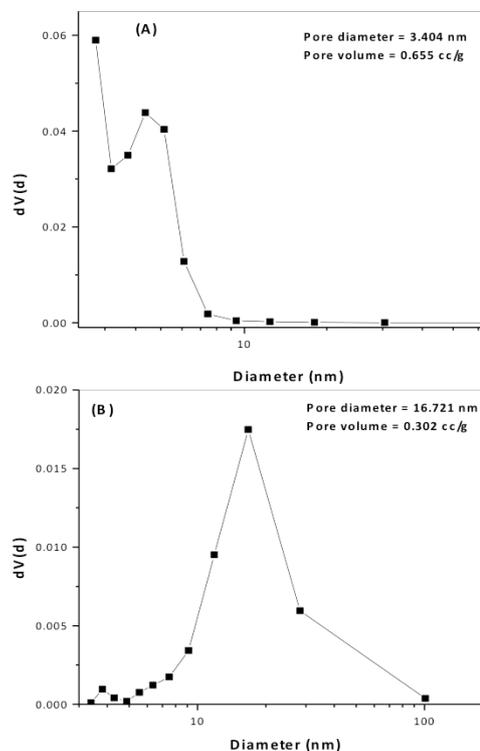
$$D = k\lambda/\beta\cos\theta \qquad (1)$$

where D is the average crystallite size, k is the shape factor (0.9), λ is the wavelength of X-ray radiation, *β* is the full line width at half-maxima (FWHM) of the main diffraction peak and θ is the Bragg angle of the corresponding diffraction peak (Pal *et al.*, 2014).

The weight fraction of anatase and rutile contents in the samples were calculated according to the following equations:
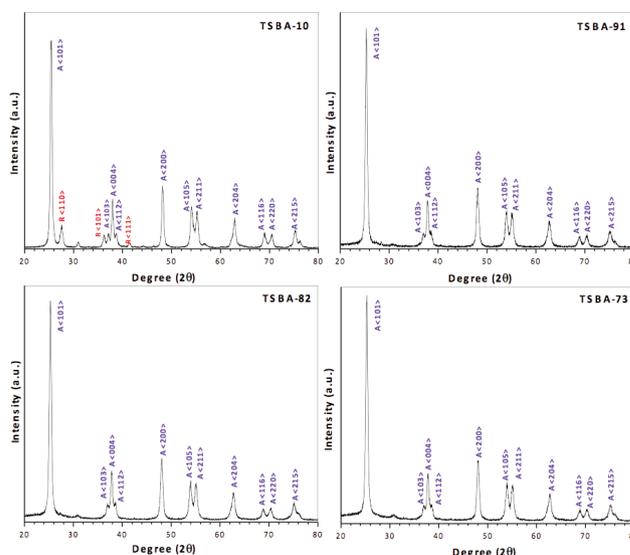

Fig. 3 - XRD spectra of the TiO₂/SiO₂ samples with different TiO₂/SiO₂ weight ratio.

$$W_A = 1/[1+1.26(I_{R110}/I_{A101})] \qquad (2)$$
$$W_R = 1/[1+0.8(I_{A101}/I_{R110})] \qquad (3)$$

where W_A and W_R are the weighted fraction of anatase and rutile in the mixed phase, and I_{A101} and I_{R110} are the integrated intensity of corresponding anatase (101) and rutile (110) diffraction peaks, respectively (Pal *et al.*, 2014). Phase composition and average crystallite size of the corresponding crystals are summarized in Table 1, where it is observed that TSBA-73, TSB-82 and TSBA-91 samples consist of pure anatase phase whereas in case of TSBA-10, there is a small amount of rutile phase formation (~11 wt%). These data clearly indicate that the mesoporous silica framework helps to stabilize the anatase crystalline phase and prevent the thermodynamically favoured phase transformation in to the rutile phase, as reported by Fu *et al*. (1996).

Table 1 - Anatase (W_A), and rutile (W_R) phase content in different TiO_2/SiO_2 samples and their corresponding crystalline sizes calculated from XRD data

Sample	Phase content		Crystalline size (nm)	
	W_A	W_R	$<D_A>$	$<D_R>$
TSBA-73	1	0	15.749	-
TSBA-82	1	0	15.998	-
TSBA-91	1	0	17.663	-
TSBA-10	0.887	0.111	17.553	13.866

FTIR measurements were carried out to investigate the bonding of SiO_2 and TiO_2 network and they are showed in figure 4. As a reference of pure silica, an FTIR spectrum of SBA is also presented. All the spectra, except for the sample TSBA-10 (100 wt% TiO_2), show intense and distinct vibrational bands at 1092, 805 and 472 cm^{-1} which are assigned to the asymmetric stretching of Si-O-Si (1092 cm^{-1}), Si-O-Si symmetric stretching (805 cm^{-1}), Si-O-Si bending vibration mode (474 cm^{-1}). The broad band around 3300-3600 cm^{-1} and the band at 976 cm^{-1} are attributed to the stretching vibration of H-bonded silanols (Si-OH) with hydroxyl groups of the adsorbed water molecules. Another peak of the adsorbed water is located at the wavenumber of 1634 cm^{-1} due to bending vibration of O-H groups. Furthermore, from the spectra it can be observed that the band at 665 cm^{-1} is absent in SBA sample, whereas it is present in all samples containing TiO_2 and it is therefore attribuited to the Ti-O bond. The appearance of broad band at 450-800 cm^{-1} range is also attributed to the presence of TiO_2 It is also interesting to see that the vibrational band at 1092 cm^{-1}, due to asym-
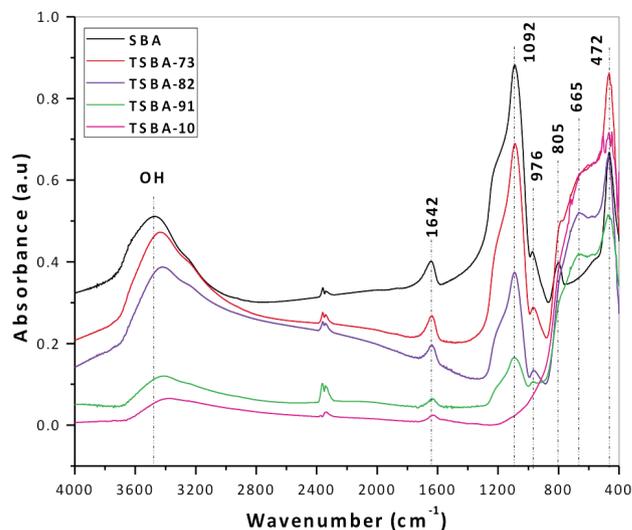

Fig. 4 - FTIR spectra of pure mesoporous silica and of the TiO_2/SiO_2 binary systems.

metric stretching of Si-O-Si, is gradually decreasing with increasing TiO_2 content in the mixed composite that confirms the variation of TiO_2/SiO_2 ratio.

FESEM measurements on two different samples, one without silica support (TSBA-10) and the other with silica support (TSBA-82) were carried out to investigate the effect of silica insertion in the composite catalyst samples. FESEM images of these two samples are showed in figure 5. The lower magnification images (Fig. 5 a, c) of TSBA-10 and TSBA-82 samples represent the overall structure of these powder samples. Whereas from the images in figure 5 (b, d), it is clearly visible the mesoporous structures. The crystallite size as estimated from the XRD spectra (Table 1) of the corresponding samples matches well with the size as observed in the FESEM images (Fig. 5 b, d).

The photocatalytic efficiency of the powder samples was evaluated by the photo-oxidation of ethylene under UV light illumination. The percentage of ethylene photo-oxidation with reaction time under UV light corresponding to four catalysts is summarized in Table 2. For a better comparison, data reported in Table 2 have been presented as histogram in figure 6. From Table 2 and figure 6, it is clear that the overall photo-oxidation efficiency of TSBA-82 sample is higher respect to the others. It also shows a superior catalytic activity in early reaction times. The higher catalytic activity of TSBA-82 sample can be explained owing to stable anatase crystalline phase, higher specific surface area and having optimum amount of mesoporous silica support.
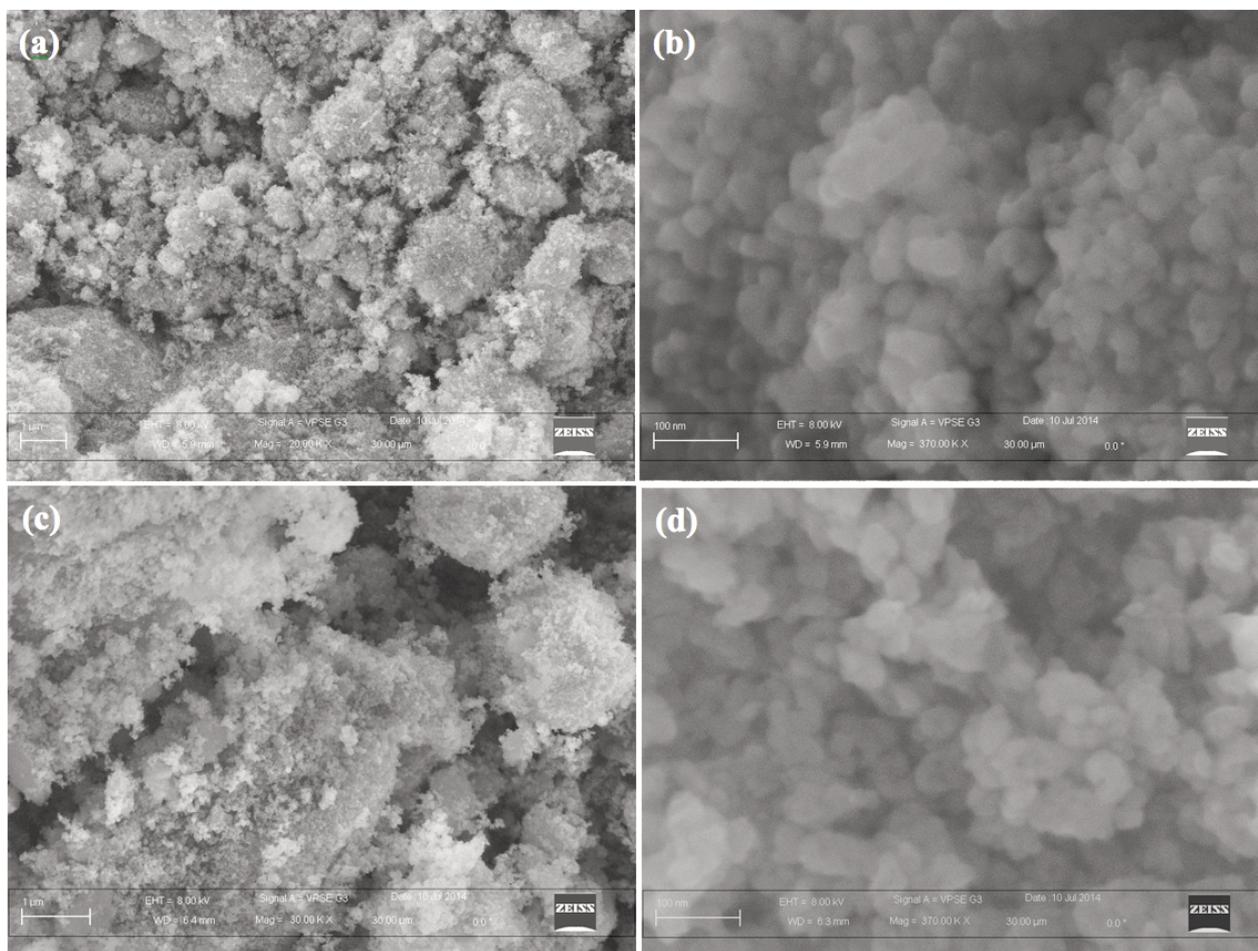
Fig. 5 - FESEM images of (a, b) TSBA-10 and (c, d) TSBA-82 samples.

Table 2 - Percentage of oxidized ethylene for the catalysts TSBA-10, TSBA-91, TSBA-82, and TSBA-73 as a function of the UV light irradiation

Time (h)	Oxidized ethylene (%)			
	TSBA-10	TSBA-91	TSBA-82	TSBA-73
0	0	0%	0%	0%
1	2%	0%	6%	8%
2	8%	5%	15%	6%
3	16%	15%	20%	8%
4	22%	22%	25%	11%
5	26%	31%	30%	13%
24	98%	97%	99%	89%

Fig. 6 - Histogram showing the ethylene oxidation efficiency of four catalyst samples with the reaction time under UV light exposure.

4. Conclusions

TiO₂/SiO₂ catalysts, with different TiO₂/SiO₂ weight ratios, were synthesized by liquid crystal template technique, being SiO₂ the mesoporous support
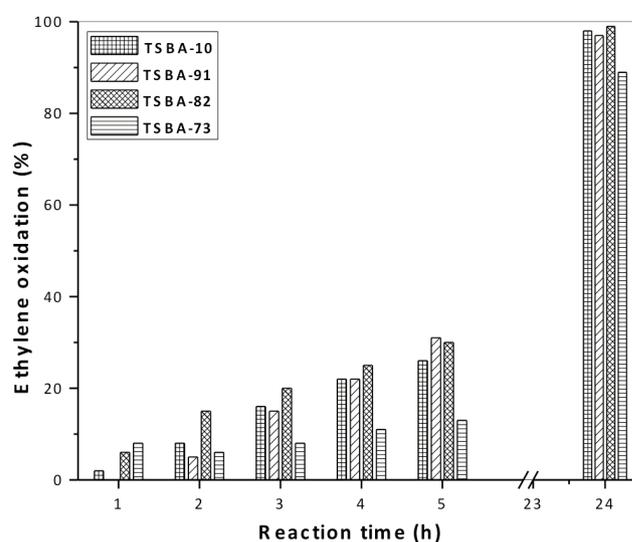
of TiO₂ catalyst. XRD results prove that a more stable anatase phase with silica insertion even at higher calcination temperature is obtained. Increasing the silica content also leads to a higher specific surface area. FESEM images showed the well-defined structure of the catalyst samples. The photocatalysis experiments revealed that, after 24 hours of reaction under UV light, total oxidation of ethylene was achieved in case of TSBA-82 catalyst. The other catalysts, such as, TSBA-0 and TSBA-91 also showed interesting results but the highest activity was observed with the TSBA-82 sample. This higher efficiency was explained with surface area, phase stability and optimum mesoporous support. Overall it can be stated that the TiO₂/SiO₂, rather than pure TiO₂ is a promising candidate in photocatalytic degradation of ethylene. It is therefore expected that TiO₂/SiO₂ can be fruitfully used in several applications requiring the control of ethylene to prevent ripening of fruits and vegetables.

Acknowledgements

References

BECK J.S., VARTULLI J.C., ROTH W.J., LEONOWICZ M.E., KRESGE C.T., SCHMITT K.D., CHU C.T.W., OLSON D.H., SHEPPARD E.W., MCCULLEN S.B., HIGGINS J.B., SCHLENKER J.L., 1992 - *A new family of mesoporous molecular sieve prepared with liquid crystal templates*. - J. Am. Chem. Soc., 114: 10834-10843.

CORMA A., DIAZ-CABANES M.J., MOLINER M., RODRIGUEZ G., 2006 - *Synthesis of micro- and mesoporous molecular sieves at room temperature and neutral pH catalysed by functional analogues of silicatein*. - Chem. Comm., 29: 3127-3139.

FU X., CLARK L.A., YANG Q., ANDERSON A., 1996 - *Enhanced photocatalytic performance of titania-based binary metal oxide: TiO₂/SiO₂ and TiO₂/ZriO₂*. - Environ. Sci. Technol., 30: 647-653.

HUSSAIN M., BENSAID S., GEOBALDO F., SARACCO G., RUSSO N., 2011 - *Photocatalytic degradation of ethylene emitted by fruits with TiO₂ nanoparticles*. - Ind. Eng. Chem. Res., 50: 2536-2543.

KELLER N., DUCAMP M.N., ROBERT D., KELLER V., 2013 - *Ethylene removal and fresh product storage: A challenge at the frontiers of chemistry. Toward an approach by photocatalytic oxidation*. - Chem. Rev., 113: 5029-5070.

PAL S., LAERA A.M., LICCIULLI A., CATALANO M., TAURINO A., 2014 - *Biphase TiO₂ microspheres with enhanced photocatalytic activity*. - Ind. Eng. Chem. Res., 53: 7931-7938.

PARK D.R., ZHANG J., IKEUE K., YAMASHITA H., ANPO M., 2009 - *Photocatalytic oxidation of ethylene to CO₂ and H₂O on ultrafine powdered TiO₂ photocatalysts in the presence of O₂ and H₂O*. - J. Catal., 185: 114-119.

XIAO Q., WANG J., ZHOU H., SUN P., YUAN Z., LI B., DING D., CHEN T., 2008 - *Low temperature effect on the morphological control of* mesoporous silican *nanofibers at near-neutral pH: a biomimetic strategy.* - Micropor. Mesopor. Mat., 109: 233-238.

YE S.Y., FANG Y.C., SONG X.L., LUO S.C., YE L.M., 2013 - *Decomposition of ethylene in cold storage by plasma-assisted photocatalyst process with TiO₂/ACF-based photocatalyst prepared by gamma irradiation*. - Chem. Eng. J., 225: 499-508.

ZHAN C., CHEN F., YANG J., DAI D., CAO X., ZHONG M., 2014 - *Visible light responsive sulphated rare earth doped TiO₂@fumed SiO₂ composites with mesoporosity: enhanced photocatalytic activity for methyl orange degradation.* - J. Hazard. Mater., 267: 88-97.